Supporting Information

Support effect–induced electronic modulation facilitates ammonia desorption on Co_3O_4/NF for enhanced nitrate reduction

Shuang Yuan[a], Lewa Zhang[b], Huidong Du[a], Chenyuan Zhu[b], Hongtao Xie*[b,c], Yali Cao*[a], Jianping Sheng[b], and Yizhao Li*[a,b]

[a] *State Key Laboratory of Chemistry and Utilization of Carbon Based Energy Resources; College of Chemistry, Xinjiang University, Urumqi 830017, P.R. China.*

[b] *Huzhou Key Laboratory of Smart and Clean Energy, Yangtze Delta Region Institute (Huzhou), University of Electronic Science and Technology of China, Huzhou 313001, China.*

[c] *Carbon Neutral Institute, China University of Mining and Technology, Xuzhou 221008, China.*

[*] *Corresponding author. Tel: +86-991-8583083; Fax: +86-991-8588883; E-mail address: xieht@cumt.edu.cn (H. Xie); caoyali523@163.com (Y. Cao); yizhao@csj.uestc.edu.cn (Y. Li).*

Experimental section:

Materials: All chemical reagents used in this study were purchased from Aladdin (analytical grade).

Synthesis of Co_3O_4/NF: Prior to synthesis, Ni foam was ultrasonically cleaned successively in 1 M HCl, ethanol, and deionized water for 30 min each to remove surface oxides and impurities, followed by drying at room temperature. Typically, 80 mg of cobalt(II) acetylacetonate was dissolved in 100 mL of ethanol under ultrasonication to obtain a homogeneous purple-red precursor solution. The pretreated Ni foam was immersed in the precursor solution for approximately 10 s, taken out, and allowed to drain briefly to remove excess solution. Subsequently, the precursor-wetted Ni foam was placed in the outer flame region of an alcohol lamp using clean tweezers. The distance between the Ni foam and the outer flame was maintained at approximately 1 cm. Each combustion process lasted for approximately 30 ± 5s until the ethanol absorbed on the Ni foam was completely burned off. After each combustion step, the sample was naturally cooled to room temperature before the next immersion–combustion cycle. The above immersion–combustion process was repeated 15 times to obtain Co_3O_4/NF. The synthesis was carried out under ordinary laboratory ambient conditions, with a room temperature of approximately 25 °C and a relative humidity of approximately 75 ± 10%. No additional temperature or humidity control was applied during the synthesis. The synthesis procedures of Co_3O_4/CF and Co_3O_4/IR were carried out using a similar method. Specifically, CF refers to cobalt foam, and IR refers to iron foam.

Preparation of electrodes:

Co_3O_4/CC: To prepare the catalyst-coated carbon paper electrode, 10 mg of Co_3O_4 powder was dispersed in 0.8 mL deionized water and 0.2 mL isopropanol, followed by the addition of 50 μL of 5 wt% Nafion. The mixture was ultrasonicated for 1 hour until the catalyst was uniformly dispersed. The resulting catalyst ink was then evenly drop-cast onto one side of a 1 × 1 cm^2 carbon paper. Specifically, CC refers to carbon cloth.

Electrochemical measurements: Electrochemical measurements were carried

out using a CHI 760E electrochemical workstation (CH Instruments, Shanghai, China). A platinum plate was used as the counter electrode, and a saturated calomel electrode (SCE) served as the reference electrode. All potentials were calibrated with respect to the reversible hydrogen electrode (RHE) according to the following equation: $E_{vs\ RHE} = E_{vs.\ SCE} + E_{SCE} + 0.059\ pH$.

The linear sweep voltammetry (LSV) measurements were conducted at a scan rate of 10 mV/s. All current densities were normalized to the geometric area of the electrodes. Argon was used as the carrier gas with a flow rate of 20 sccm.

Preparation of standard curves and quantification of ammonia production:

Solution A: 4 g NaOH, 5.778 g of salicylic acid and sodium citrate, and 100 mL of water were combined and stored in a large black plastic bottle.

Solution B: 1.772 mL of NaClO solution with 4% active chlorine was diluted to 20 mL to obtain 0.05 M NaClO solution, preferably stored in a brown bottle.

Solution C: 0.1 g (1 wt%) sodium nitroprusside was added to 9.9 mL water in a 10 mL transparent bottle.

Preparation of NH_4Cl standard solutions: Weigh 50 mg NH_4Cl and dissolve in electrolyte in a 50 mL volumetric flask to prepare a 1 mg/mL stock solution. Take 0.5 mL of the stock solution and dilute to 10 mL to obtain 0.05 mg/mL. Prepare a series of standard solutions by taking 0, 40, 80, 160, 240, 320, and 400 μL of the 0.05 mg/mL solution and diluting to 2 mL with electrolyte, resulting in concentrations of 0, 1, 2, 4, 6, 8, and 10 μg/mL. The x-axis of the calibration curve corresponds to the NH_4Cl concentration; it can be converted to NH_4^+ mass concentration. More concentrated standard solutions can also be prepared if needed.

Color development: To each 2 mL of standard solution, add 2 mL of Solution A, 1 mL of Solution B, and 0.2 mL of Solution C; allow color development in the dark for 30 min.

UV-Vis measurement: Scanning was performed using the new method with a wavelength range of 550-750 nm, absorbance 0-2, medium speed, and baseline correction. Electrolyte was used as the blank baseline for all measurements.

NO_2^-: Calibration curve preparation and product detection

Color developing reagent preparation: A brown solution was prepared by dissolving 0.1 g N-(1-naphthyl)-ethylenediamine dihydrochloride, 1 g sulfanilamide, and 2.94 mL H_3PO_4 in 50 mL of water.

Preparation of NO_2^- standard solutions: 50 mg of $NaNO_2$ (MW: 69 g/mol) was dissolved in electrolyte and diluted to 50 mL. Then, 0.5 mL of this solution was further diluted to 10 mL in a centrifuge tube (0.05 mg/mL). From this, 0, 40, 80, 120, 160, and 200 μL were transferred into separate glass vials and diluted with electrolyte to a final volume of 1 mL, resulting in final concentrations of 0, 2, 4, 6, 8, and 10 μL/mL.

Color development and measurement: For each 1 mL standard solution, 2 mL water and 1 mL color developing reagent were added. After 10 min of color development, UV-Vis measurement was performed. The calibration curve x-axis corresponds to $NaNO_2$ concentration, which can be converted to NO_2^- mass concentration; higher-concentration standard solutions can also be prepared. The order of addition is: electrolyte + water + color reagent.

UV-Vis measurement: Scanning was performed using the new method with a wavelength range of 450-650 nm, absorbance 0-2, medium speed, and baseline correction. Electrolyte was used as the blank baseline for all measurements.

DFT Calculations: The exchange-correlation potential is described by using the generalized gradient approximation of Perdew-Burke-Ernzerhof (GGA-PBE). The projector augmented-wave (PAW) method is employed to treat interactions between ion cores and valence electrons. The plane-wave cutoff energy was fixed to 450 eV. Given structural models were relaxed until the Hellmann–Feynman forces smaller than -0.02 eV/Å and the change in energy smaller than 10-5 eV was attained. Grimme's DFT-D3 methodology was used to describe the dispersion interactions among all the atoms in adsorption models. The Gamma-centered k-points samplings were set to 2 × 2 × 1 for modle. The vacuum space along the z-direction was set to be 14 Å. The Gibbs free energy change is defined as:

$$\Delta G = \Delta E + \Delta ZPE - T\Delta S$$

where ΔE is the electronic energy, ΔZPE and ΔS are the zero-point energy difference and the entropy change between the products and reactants, respectively, and T is the

temperature (298.15 K).

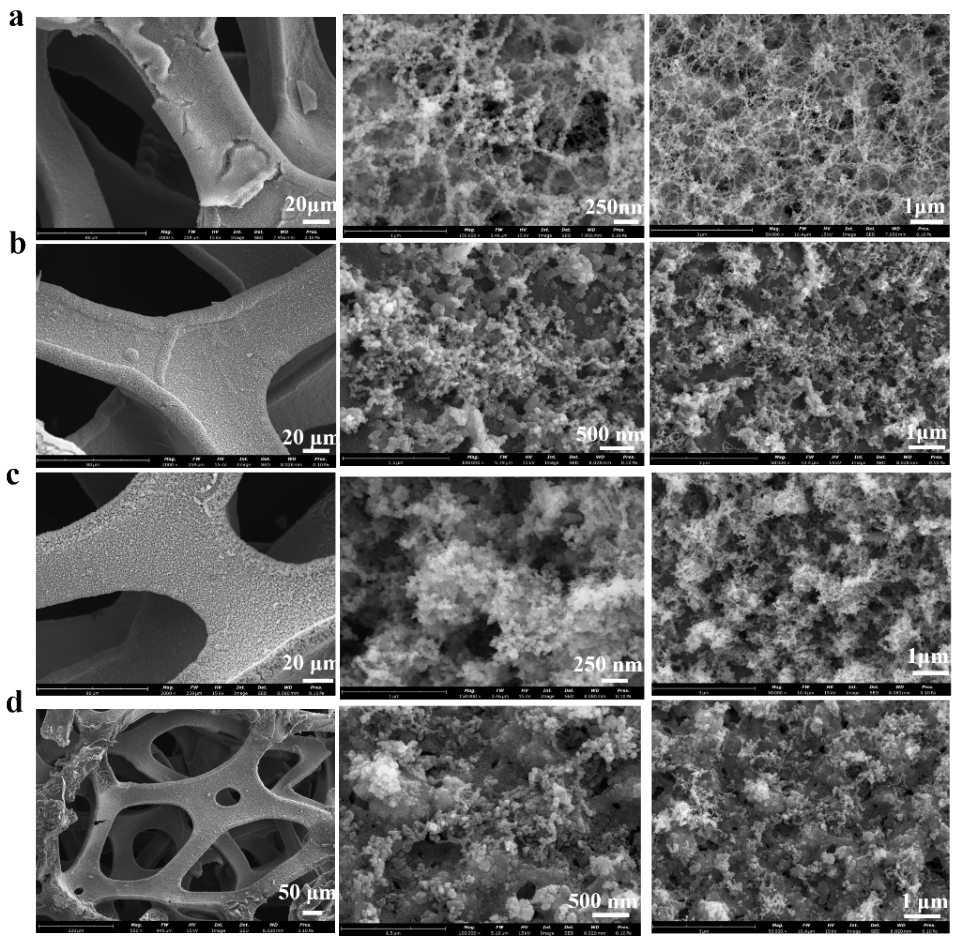

Fig. S1 Scanning electron microscopy (SEM) images of Co_3O_4 after varying numbers of calcination treatments: (a-d) Correspond to 5, 10, 15, and 20 calcination cycles, respectively.

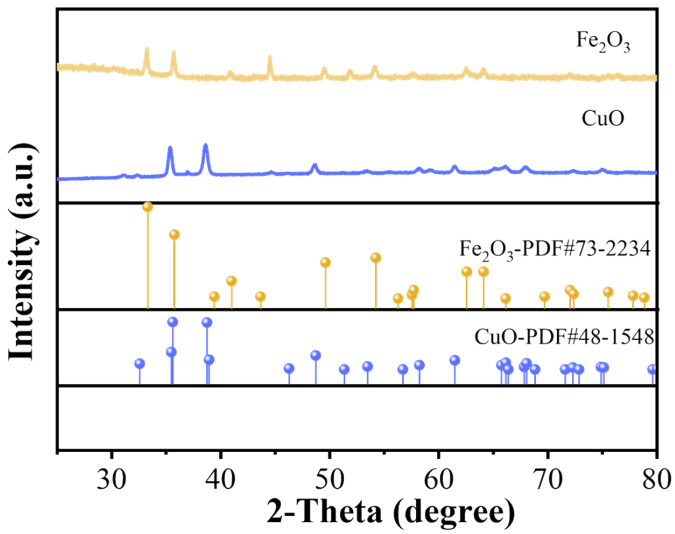

Fig. S2 XRD patterns of different samples.

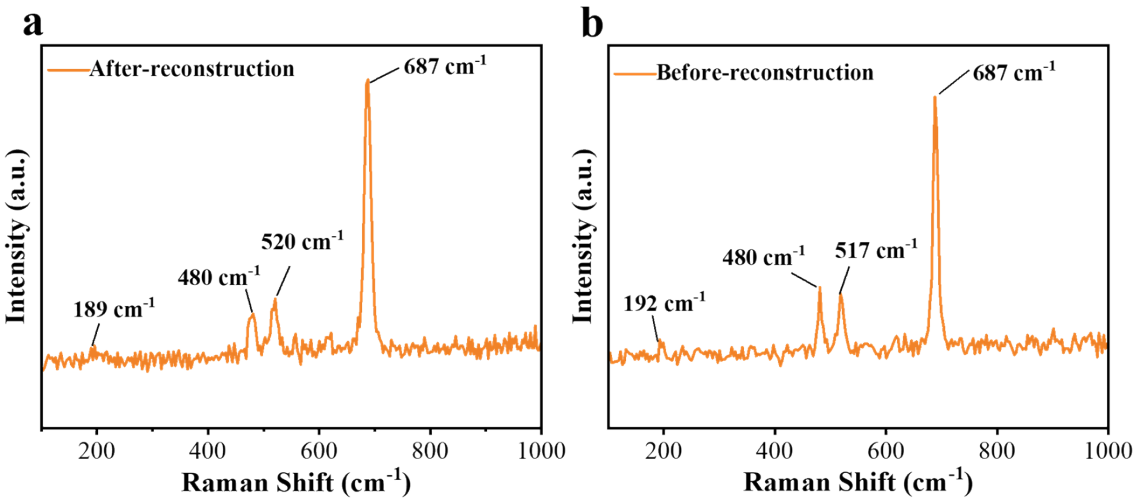

Fig. S3 The Raman spectra of Co_3O_4/NF.

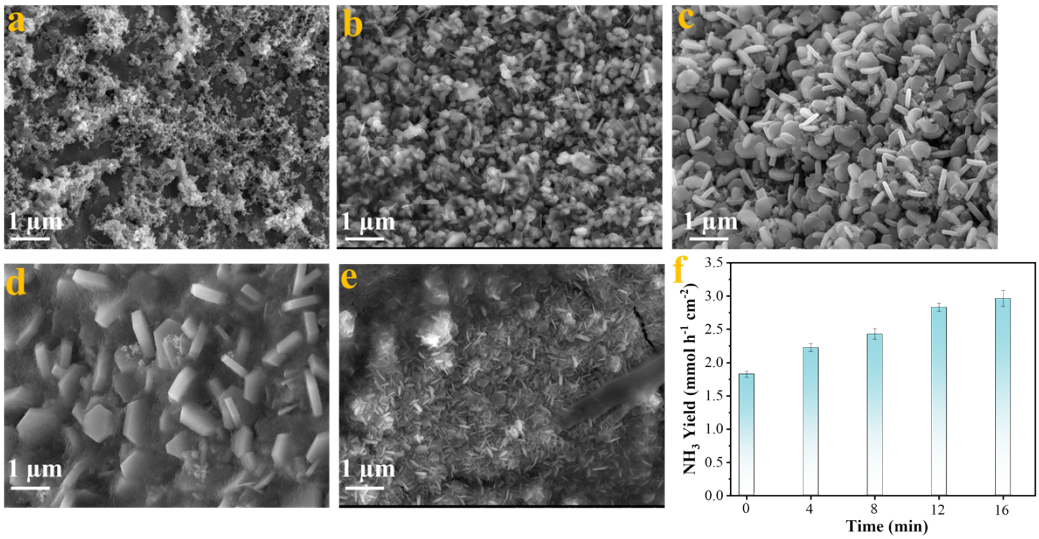

Fig. S4 SEM images of the catalysts after different activation times: (a-e) correspond to activation times of 0, 4, 8, 12, and16 min, respectively; (f) shows the corresponding ammonia production rates.

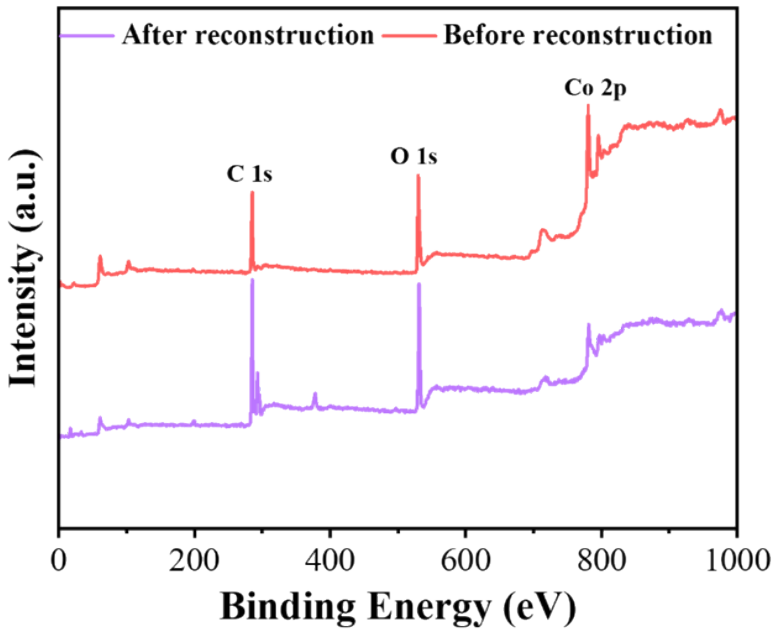

Fig. S5 XPS survey spectra of Co_3O_4/NF.

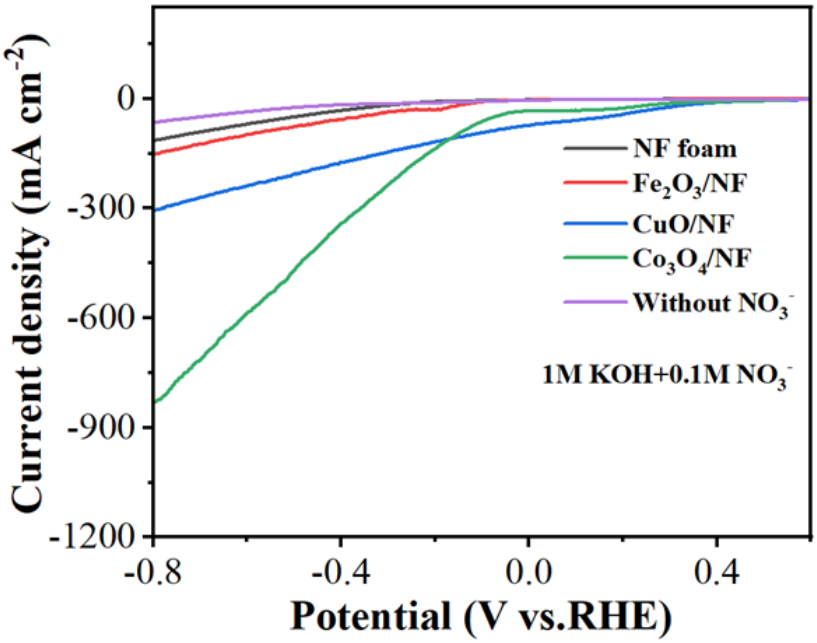

Fig. S6 LSV curves of different samples.

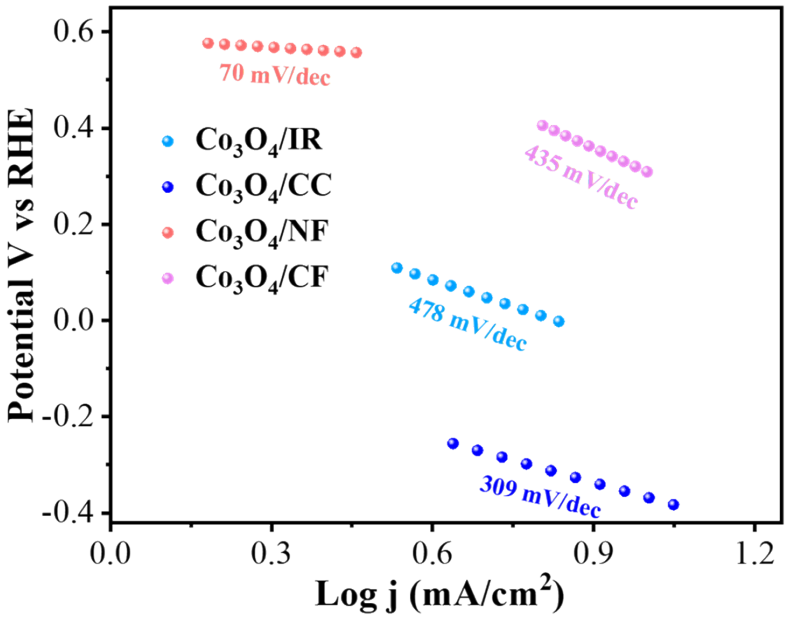

Fig. S7 Tafel plots of various samples.

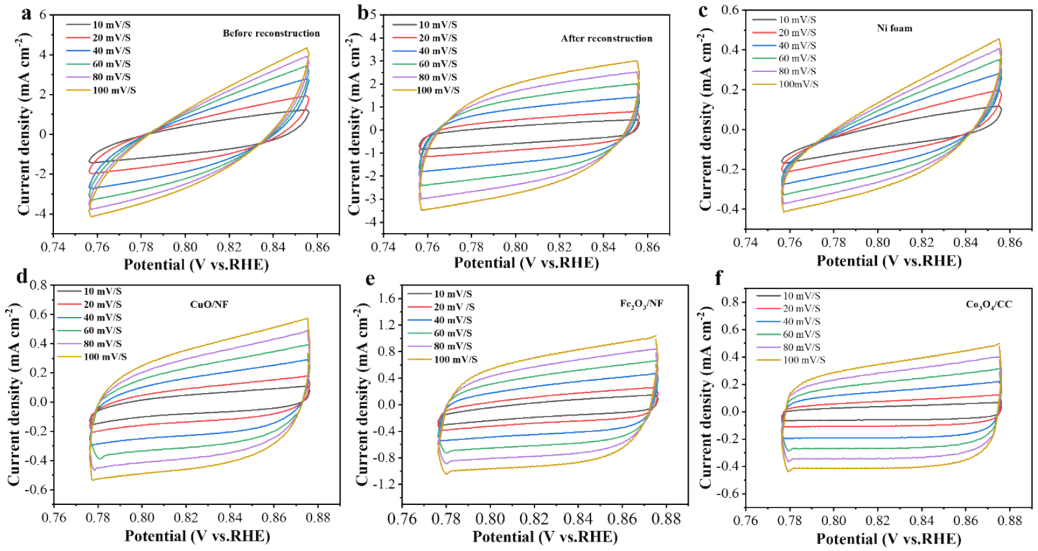

Fig. S8 Cyclic voltammograms of (a) before reconstruction Co_3O_4/NF, (b) after reconstruction Co_3O_4/NF and (c) NF (d) CuO/NF, (e) Fe_2O_3/NF, (f) Co_3O_4/CC recorded at scan rates of 10, 20, 40, 60, 80 and 100 mV s^{-1} in the double-layer region (0.76-0.86 V vs. RHE). The nearly symmetric rectangular profiles indicate ideal capacitive behaviour.

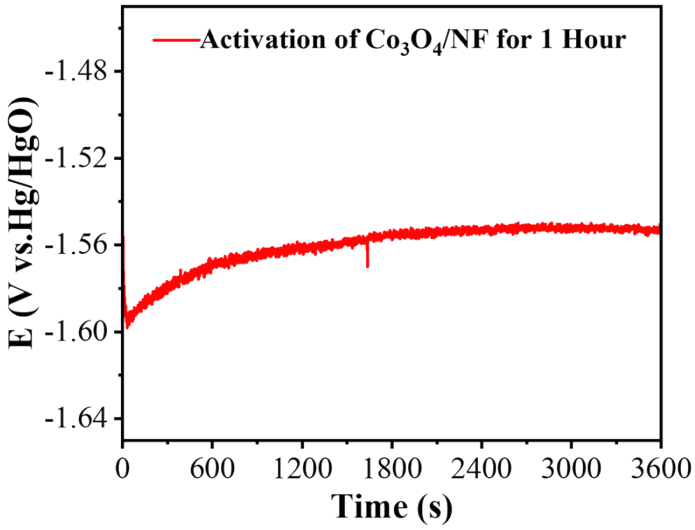

Fig. S9 The i-t curves of the Co_3O_4/NF electrode was activated for 1 hour.

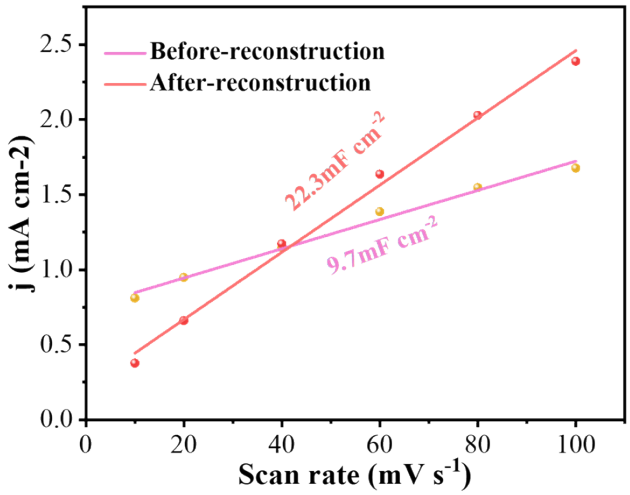

Fig. S10 Double-layer capacitance (C_{dl}) values before and after the reconstruction.

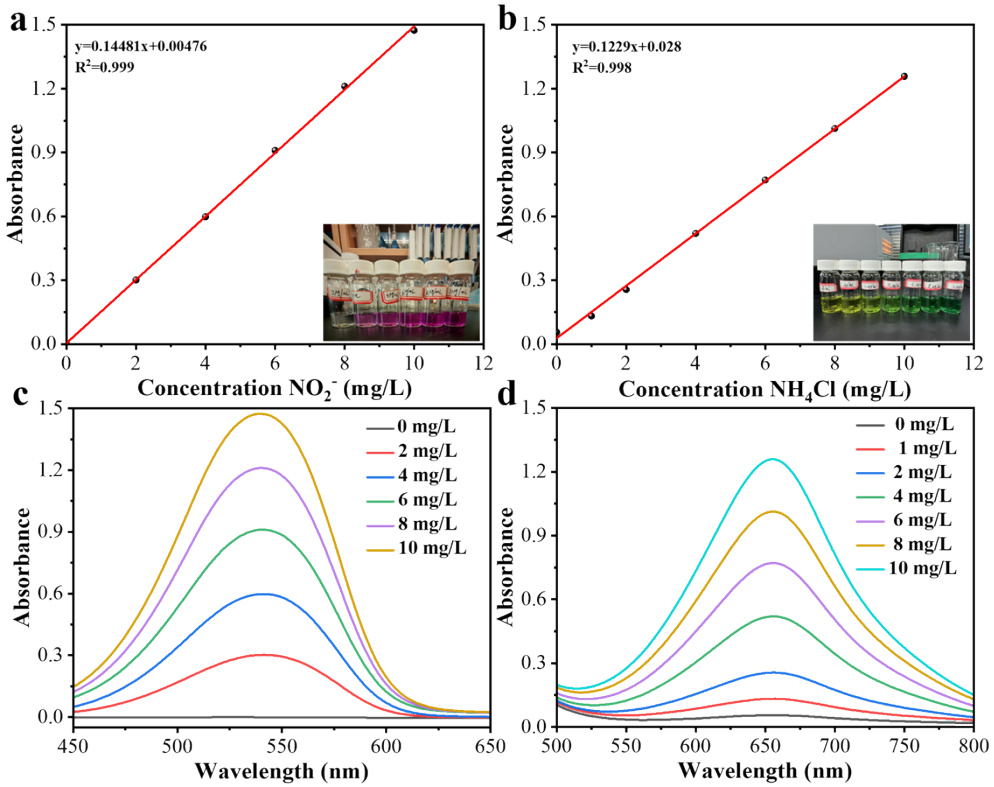

Fig. S11 (a) Calibration curve of NO_2^-, (b) calibration curve of NH_4^+, and (c, d) the corresponding UV-Vis absorption spectra of NO_2^- and NH_4^+, respectively.

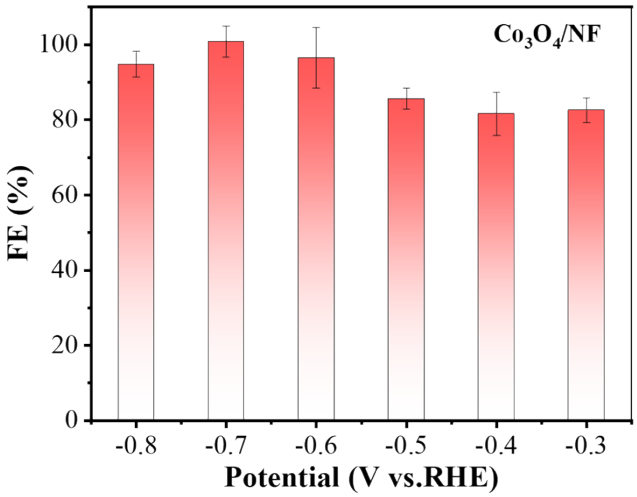

Fig. S12 FE of Co_3O_4/NF.

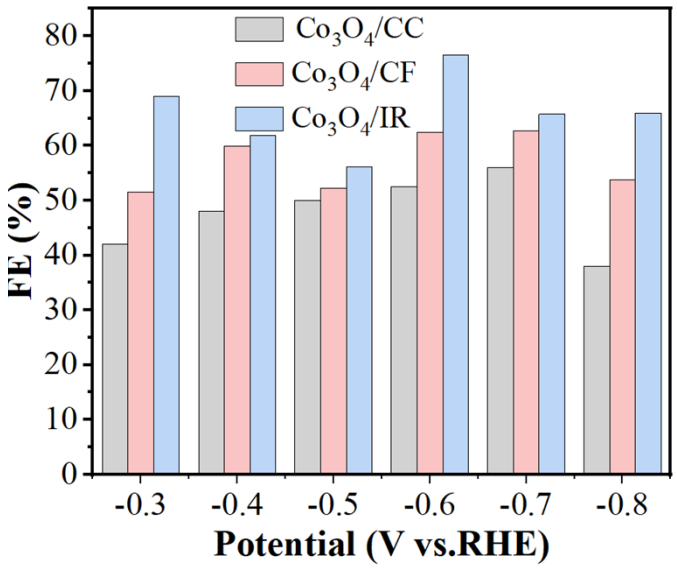

Fig. S13 Faradaic efficiency of Co_3O_4 on different supports.

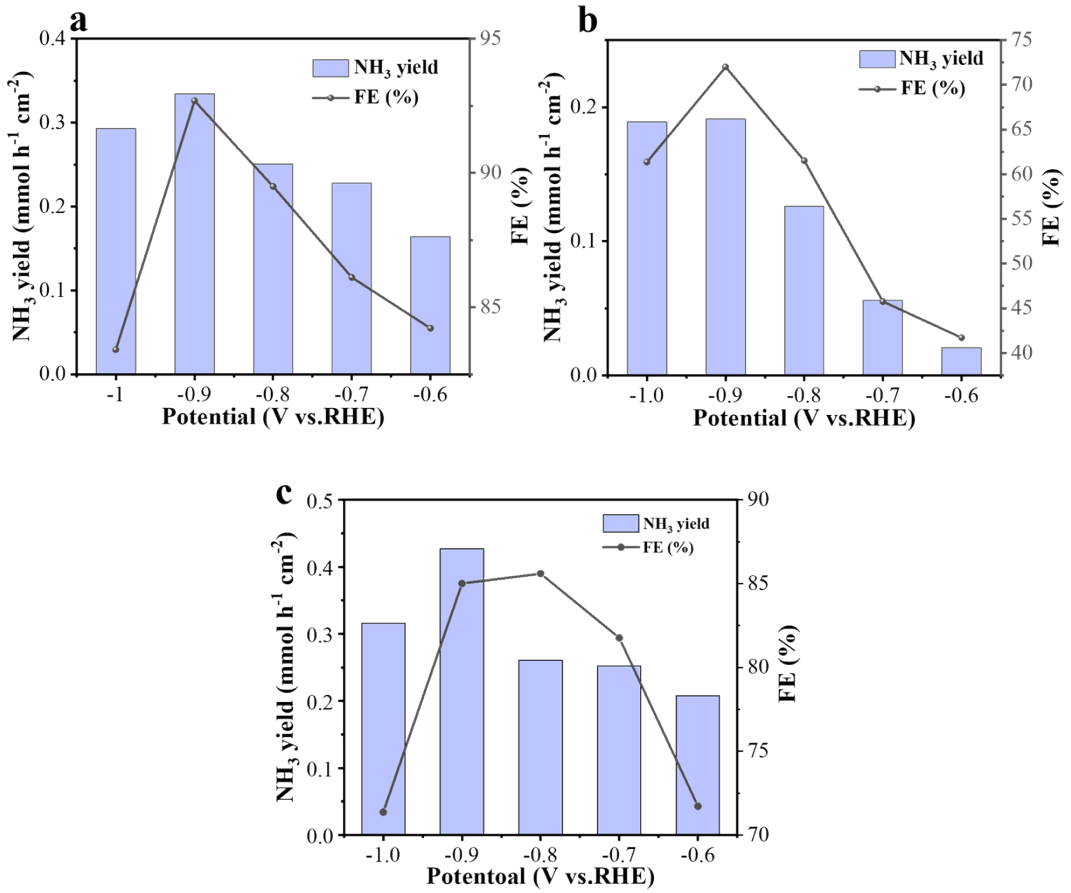

Fig. S14 (a-c) Electrochemical performance of Co_3O_4/NF in 0.1M Na_2SO_4+0.1M KNO_3 electrolyte with different calcination cycles (5, 10, and 15 times).

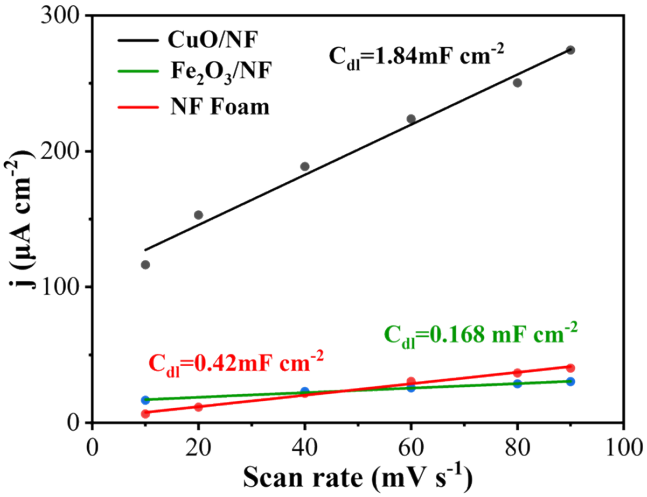

Fig. S15 Different samples exhibited varying C_{dl} values, indicating differences in their electrochemical surface areas.

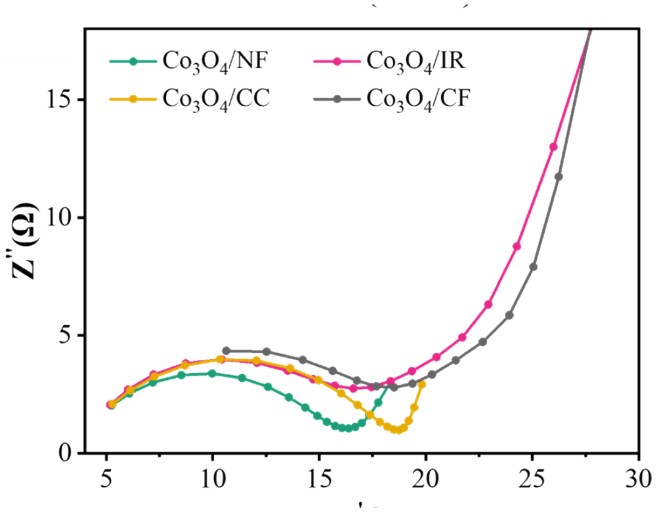

Fig. S16 The equivalent circuit diagram of Co_3O_4 on different supports.

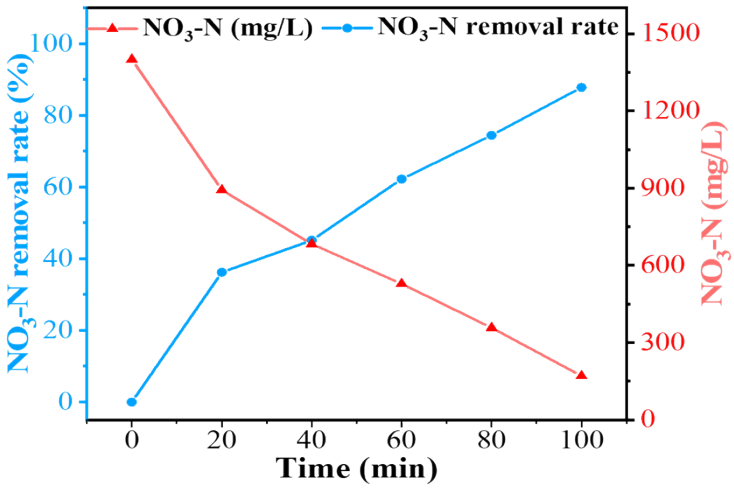

Fig. S17 Nitrate removal efficiency in 0.1 M NO_3^- solution.

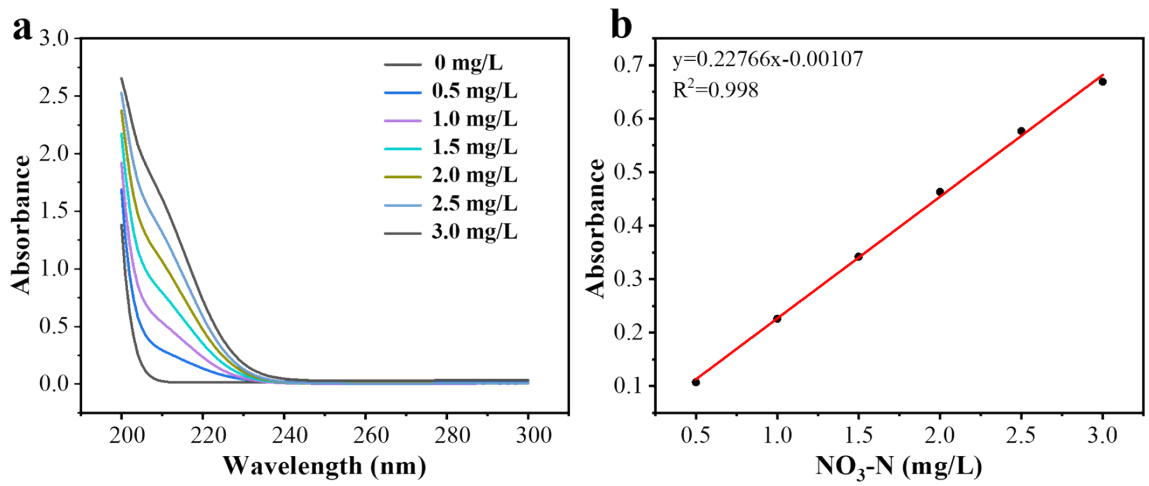

Fig. S18 The NO_3^- concentration was determined using a standard calibration curve.

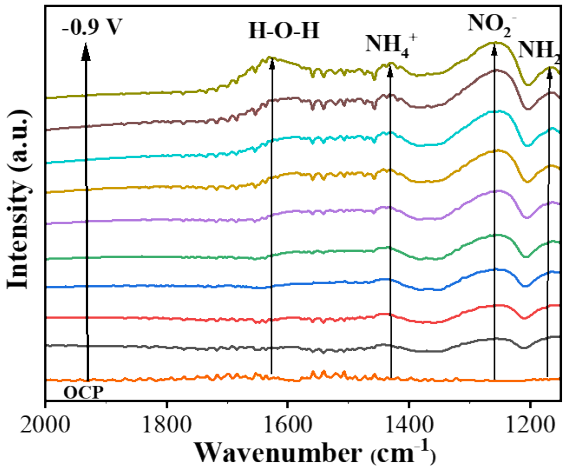

Fig. S19 In situ FTIR spectra of Co_3O_4.

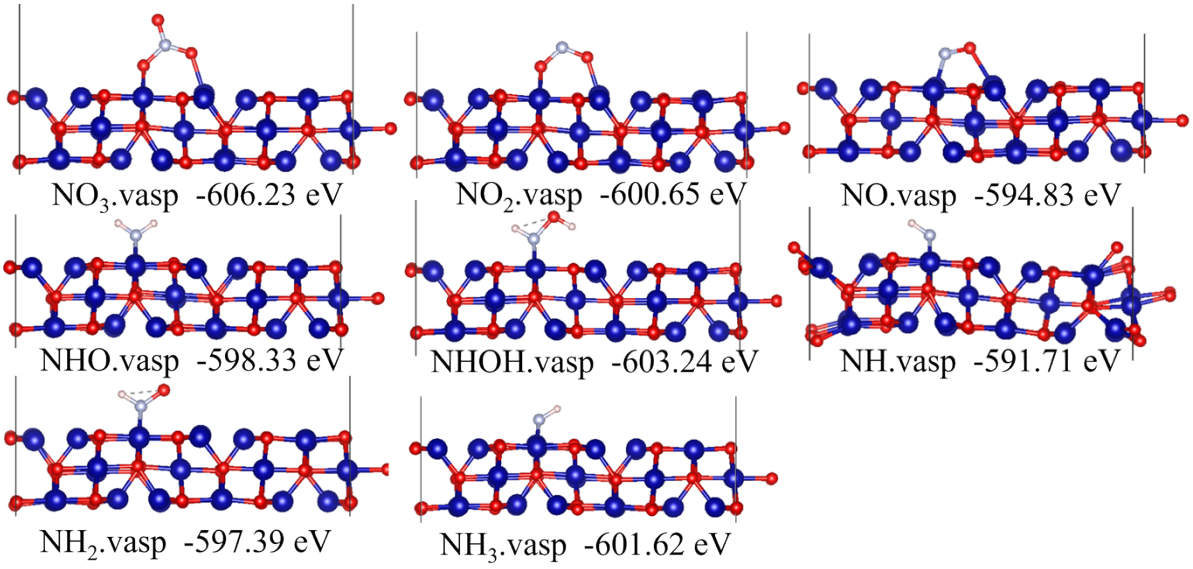

Fig. S20 The theoretical calculation model of Co_3O_4.

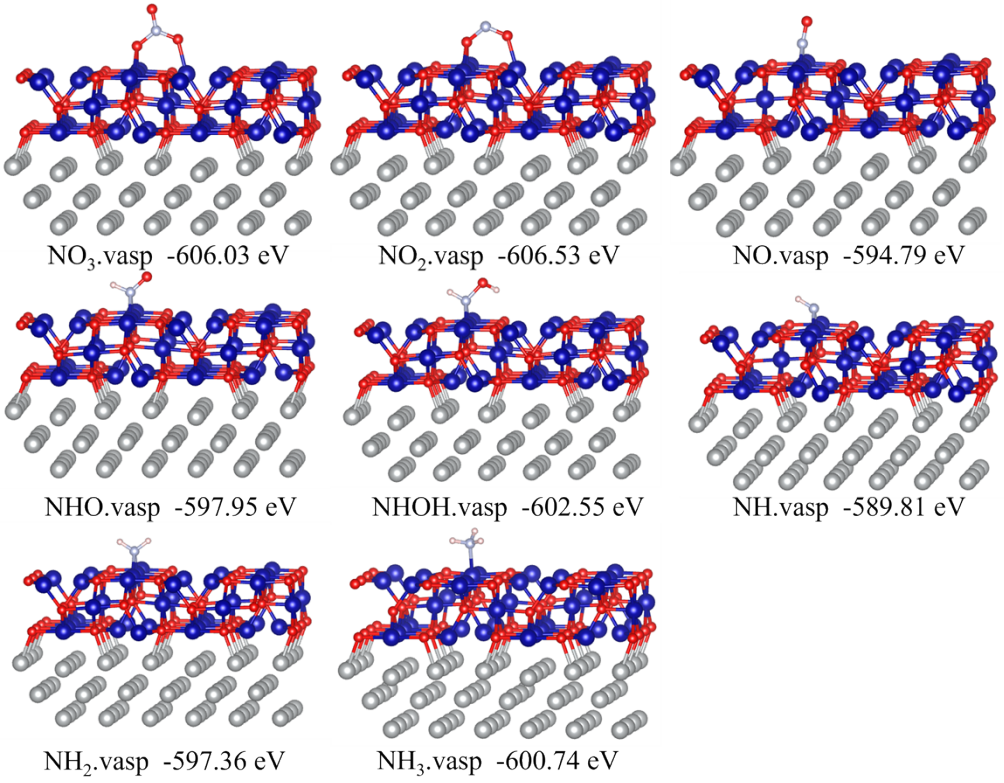

Fig. S21 The theoretical calculation model of Co_3O_4/NF.

Table S1 The NO_3RR performance of electrocatalysts in previous literature.

Catalyst	Electrolyte	pH	Potential (V vs. RHE)	NH_3 yield (mmol h^{-1} cm^{-2})	FE	Ref.
$(FeCoNiCu)O_x/CeO_2$	0.1M KNO_3 + 0.1M KOH	13	-0.4	1.782	90%	1
$Co(OH)_2/Bi_{12}O_{17}Br_2$	0.1M KNO_3 + 1M KOH	14	-0.4	1.459	93.3%	2
CoFe-cMOFs	0.1M KNO_3 + 1 M Na_2SO_4	7	-0.7	0.829	94.3%	3
c-Co@a-Cu	0.1M Na_2SO_4+0.05 M $NaNO_3$	7	-0.6	0.272	99.6%	4
Ru-$Ni(OH)_2$	0.1M KNO_3 + 1M KOH	14	-0.3	1.324	Nearly 100%	5
CuCoSP	0.1M KNO_3 + 1M KOH	14	-0.175	1.17	93.3%	6
D-Cu-Co_3O_4	0.1M KNO_3 + 1M KOH	14	-0.4	2.368	96.4%	7
Co_3O_4/NF	0.1M KNO_3 + 1M KOH	14	-0.7	2.96	Nearly 100%	This work

Supplementary references

1. Y. Qie, J. Gao, S. Li, M. Cui, X. Mao, X. Wang, B. Zhang, S. Chi, Y. Jia, Q.-H. Yang, C. Yang and Z. Weng, *Science China Materials*, 2024, **67**, 2941-2948.

2. S. Tian, R. Wu, H. Liu, C. Yan, Z. Qi, P. Song, W.-J. Chen, L. Song, Z. Wang and C. Lv, *Angew. Chem*., 2025, **64**, e202510665.

3. J. Wei, Y. Liu, Z. Wu, L. Han, A. Deng, Q. Li, C. Jiang, J. Liu, L. Gan, Y. Zhang and S. Wang, *Adv. Funct. Mater*., 2025, **32**, e13566.

4. L. Yu, J. Mu, H. Liu, G. Liao, B. Li, Y. Xia, Z. Wang, J. Yuan, J. Shen and C. Liu, *Adv. Funct. Mater*., 2025, **35**, 2424119.

5. Y. Wan, M. Pei, Y. Tang, Y. Liu, W. Yan, J. Zhang and R. Lv, *Adv.Mater*., 2025, **37**, 2417696.

6. W. Gao, Z. Yan, S. Tian, J. Cui, B. Xie, Q. Jiao, C. Zhong and J. Liu, *Applied Catalysis B: Environment and Energy*, 2025, **377**, 125495.

7. W. He, J. Zhang, S. Dieckhöfer, S. Varhade, A. C. Brix, A. Lielpetere, S. Seisel, J. R. C. Junqueira and W. Schuhmann, *Nat.Commun.,* 2022, **13**, 1129.